Neurochemistry International 128 (2019) 106–114

Contents lists available at ScienceDirect

Neurochemistry International

journal homepage: www.elsevier.com/locate/neuint

Activation of liver x receptors prevents the spinal LTP induced by skin/muscle retraction in the thigh via SIRT1/NF-Kb pathway

Xiongxiong Zhong[a,1], Wei Wang[a,1], Zuchao Mao[a], Feng Gao[a], Ruixian Guo[a,b], Xuxia Wei[c,**], Xianguo Liu[a,b], Xuhong Wei[a,b,*]

[a] Department of Physiology and Pain Research Center, Zhongshan School of Medicine, Sun Yat-sen University, Guangzhou, Guangdong, PR China
[b] Guangdong Provincial Key Laboratory of Brain Function and Disease, Guangzhou, Guangdong, PR China
[c] Department of Surgery ICU, The Third Affliated Hospital of Sun Yat-sen University, Guangzhou, Guangdong, PR China

ARTICLE INFO

Keywords:
Liver X receptor
Long term potentiation
Silent information regulator 1
Acetylated nuclear factor kappaB
Tumor necrosis factor-alpha

ABSTRACT

It has been reported that skin/muscle incision and retraction (SMIR) in the thigh, produces mechanical allodynia in the hind paw, far from the site of incision/retraction. The mechanical allodynia lasts about 22 days, indicating chronic post-operative pain develops. The precise mechanisms, however, are largely unclear. In the current study, we further found that SMIR surgery induced LTP of c-fiber evoked field potentials that lasted at least 4 h. The mRNA and protein level of tumor necrosis factor-alpha (TNFα) and acetylated nuclear factor-kappaB p65 (ac-NF-κB p65) in the lumbar spinal dorsal horn was gradually increased during LTP development, while pretreatment with either TNFα neutralization antibody or NF-κB inhibitor PDTC completely prevented the induction of LTP. Moreover, the expression of Silent information regulator 1 (SIRT1) in the lumbar spinal dorsal horn was decreased and activation of SIRT1 by SRT1720 also prevented the induction of LTP. Importantly, the spinal expression of Liver X receptors (LXRs) was increased, both at mRNA and protein level following SMIR. Application of LXRs agonist T0901317 to the spinal dorsal horn prevented LTP induction following SMIR. Mechanistically, T0901317 enhanced the expression of SIRT1 and decreased the expression of ac-NF-κB p65 and TNFα. Spinal application of SIRT1 antagonist EX-527, 30 min before T0901317 administration, completely blocked the inhibiting effect of T0901317 on LTP, and on expression of ac-NF-κB p65 and TNFα. These results indicated that activation of LXRs prevented SMIR-induced LTP by inhibiting NF-κB/TNFα pathway via increasing SIRT1 expression.

1. Introduction

It has been reported that skin/muscle incision and retraction (SMIR) in the thigh, produces chronic postsurgical pain (CPSP) in the hind paw, far from the site of incision/retraction (Flatters, 2008; Song et al., 2018; Ying et al., 2014). The underlying mechanisms, however, are still unclear. Long term potentiation (LTP) at the synapses between C-fibers and spinal dorsal horn neurons can be induced by electrical stimulation of afferent C-fibers (Liu and Sandkühler, 1997), by spinal application of adenosine triphosphate (ATP), BzATP (Kronschlager et al., 2016), brain-derived neurotrophic factor (BDNF) (Zhou et al., 2008) or remifentanil (Yang et al., 2018). Spinal LTP is considered as a cellular model of central sensitization underlying some forms of hyperalgesia (Liu and Zhou, 2015), as it is induced by noxious electrical but not by innoxious one, and that the stimulation that induce LTP, such as electrical stimulation, ATP and remifentanil, can also induce pathological pain, in human or in animals (Chu et al., 2010, 2012; Klein et al., 2007; Klein et al., 2006; Nakagawa et al., 2007; Yuan et al., 2013). Therefore, we hypothesized that SMIR surgery could also induce LTP of c-fiber evoked field potentials, and might underlie the development of CPSP following SMIR.

In unstimulated cells, nuclear factor-kappa B (NF-κB) binds to inhibitor of nuclear factor kappa-B (IκB) molecules in promoter region via its p65 subunit, which is sequestered in the cytoplasm in the inactive form. Once activated by various stimuli, IκB is dissociated via phosphorylation by the IκB kinase (IκK), and NF-κB p65 escapes from IκB

* Corresponding author. Department of Physiology and Pain Research Center, Zhongshan School of Medicine, Sun Yat-sen University, 74 Zhongshan Road 2, Guangzhou, 510080, China
** Corresponding author. Department of Surgery ICU, the Third Affliated Hospital of Sun Yat-sen University, 600 Tianhe Rd, Guangzhou, 510630, China.
E-mail addresses: maozch@mail2.sysu.edu.cn (Z. Mao), weixuxia06@163.com (X. Wei), liuxg@mail.sysu.edu.cn (X. Liu), weixhong@mail.sysu.edu.cn (X. Wei).
[1] These two authors contributed equally to 1st author.

https://doi.org/10.1016/j.neuint.2019.04.002
Received 15 January 2019; Received in revised form 3 April 2019; Accepted 5 April 2019
Available online 21 April 2019
0197-0186/

and translocates into the nucleus and induce a large number of target genes, including proinflammatory cytokines, such as TNFα (Baud et al., 2016, Peng et al., 2014; Yuan et al., 2013). P65 acetylation can result in its translocation and activation and therefore play a central role in the inflammatory and immune response. Acetylation of lysine 310, required for full activation of p65 transcription, can be deacetylated by silent information regulator 1 (SIRT1), a conserved nicotinamide adenine dinucleotide (NAD^+)-dependent deacetylase (Bagul et al., 2015, Yeung et al., 2004; Kauppinen et al., 2013). SIRT1 activation can prevent or treat neuropathic pain induced by chronic constriction injury or induced by diabetes, during which states NF-κB is activated (Lv et al., 2015; Shao et al., 2014; Yin et al., 2013; Zhou et al., 2017). Consistently, reduction of SIRT1 contributes to neuropathic pain induced by chemotherapeutic drug bortezomib (Chen et al., 2018).

Liver X receptors (LXRs) belong to the nuclear receptor superfamily. Two known different isoforms, LXRα and LXRβ have been recognized. LXRs have been unveiled to assume critical roles in formalin-induced spontaneous pain or in diabetes-induced peripheral neuropathy (Bao et al., 2017; Cermenati et al., 2012). LXRs control immune response and inflammation, by suppressing inflammatory gene expression (Dai et al., 2017; Pourcet et al., 2016). Our previous work has shown that LXRα is upregulated in spinal dorsal horn following spared nerve injury (SNI), and that intrathecal injection of LXRs agonists significantly depress the established mechanical allodynia induced by SMIR. This effect was largely attributed to LXRα′s capability to rebalance the proinflammatory and antiinflammatory cytokine, and thus inhibiting neuroinflammation (Xu et al., 2017). It has also been reported that the SIRT1/NF-κB signaling pathway mediates the protective effect of 17β-estradiol against intracerebral hemorrhage (Zheng et al., 2015) and that LXR agonist improves cardiac dysfunction in wild-type septic mice but not in SIRT1 −/− septic mice (Han et al., 2017), suggesting LXRs agonist exert protective effect via SIRT1. The interplay of LXR with SIRT1 has not been previously studied in CPSP. Therefore, the present study was designed to test whether LXRs were involved in inhibiting spinal LTP following SMIR by activating SIRT1.

2. Material and method

2.1. Animals

Male Sprague Dawley rats (200–250 g body weight) were used in the study. Animals were group-housed in a temperature-controlled room (24 ± 1 °C) and 50–60% humidity. The animals were exposed to a 12-h light/dark cycle. All studies were approved by the Sun Yat-sen University Animal Care and Use Committee (No. SYXK (yue) 2015–0107) and were carried out in accordance with the guidelines of the National Institutes of Health on animal care. All animals were randomly assigned to different treatment groups. All experiments were conducted during the daytime.

2.2. Drugs

The synthetic LXR agonist T0901317, which activates both LXRαand LXRβ, was purchased from Cayman Chemical (USA). The selective SIRT1 agonist, SRT1720 and SIRT1 antagonist EX-527 were from Selleck Chemical (Houston, TX). All of the drugs were firstly dissolved in dimethyl sulfoxide and then diluted in 0.9% saline to the appropriate concentration.

2.3. Surgery preparation and electrophysiological recording

After anesthesia with urethane (1.5 g/kg, i.p.), the rats received tracheal intubation and breathed spontaneously. The carotid artery was cannulated to monitor the mean arterial blood pressure during the electrophysiological recording, which was maintained from 80 to 120 mm Hg. To expose the lumbar enlargement of spinal cord (L4 and L5 segments), a laminectomy was carried out. The left sciatic nerve was then dissected free for electrical stimulation. After that, the skin/muscle incision surgery was carried out according to the previous studies (Flatters, 2008; Ying et al., 2014; Song et al., 2018). Briefly, a 1.5–2 cm incision was made in the skin of the medial thigh about 4 mm medial to the saphenous vein, to expose the muscle of the thigh. An incision (7–10 mm long) was then made in the superficial muscle layer of the thigh, to allow the insertion of a micro dissecting retractor (Biomedical Research Instruments Inc., Silver Spring, MD, USA).

The rats were at last placed on a stereotaxic apparatus. Warm paraffin oil (37 °C) was used to cover the exposed sciatic nerve. Colorectal temperature was kept at 37–38 °C using a heating blanket, which is feedback controlled. Recording of C-fiber evoked field potentials in spinal dorsal horn was done as described previously (Liu and Sandkuhler, 1995; Yang et al., 2018). Briefly, the left sciatic nerve was electrically stimulated with a bipolar silver chloride hook electrode, and field potentials were recorded with a tungsten microelectrode (World Precision Instruments, Sarasota, FL, USA) driven by an electronically controlled microstepping motor (Narishige Scientific Instrument Laboratory, Tokyo, Japan). The recording site was 100–500 μm deep from the surface of the spinal cord in the ipsilateral lumbar enlargement. An A/D converter card (ADC-42. PICO) was used to digitize and store data at a sampling rate of 10 kHz in the computer. The test stimuli (0.5 ms duration, at 1 min interval) delivered to the sciatic nerve was used to evoke field potentials in the spinal dorsal horn. The strength of the test stimulation was adjusted to 1.5–2 times of threshold for C- fiber response. After 30 min stable baseline recording, the skin and superficial muscle of the thigh were retracted by 2 cm carefully, during which the recording was not stopped. The retraction persisted for 1 h. The sham group of animal received skin and muscle incision but no retraction.

2.4. Western blotting

After defined survival time, the ipsilateral spinal dorsal horn of the rats was dissected and homogenized on ice in 15 mM Tris buffer (pH 7.6; 250 mM sucrose, 1 mM magnesium chloride, 1 mM dithiothreitol, 2.5 mM EDTA, 1 mM EGTA, 50 mM sodium fluoride, 10 μg/ml leupeptin, 1.25 μg/ml pepstatin, 2.5 μg/ml aprotin, 2 mM sodium pyrophosphate, 0.1 mM sodium orthovanadate, 0.5 mM phenylmethylsulfonyl fluoride, and protease inhibitor mixture; Roche Molecular Biochemicals, Switzerland). The samples were sonicated and then centrifuged at 13,000 g for 15 min. The isolated proteins were separated by sodium dodecyl sulphate-polyacrylamide gel electrophoresis (SDS-PAGE) and transferred onto a polyvinylidene fluoride (PVDF) membrane (Bio-Rad Laboratories, Inc., USA). The blots were placed in block buffer [5% nonfat milk dissolved in Tris-buffered saline (TBS) containing 50 mM Tris-HCl (pH 7.6) and 150 mM NaCl] for 1 h at room temperature, and then incubated with primary antibodies against TNFα (1:1000, Abcam, USA, catalog number: AB6671), SIRT1 (1:1000, Cell signalling Technology, USA, catalog number: 9475), acetylated-p65 antibody (1:1000; Abcam, Bristol, UK, catalog number: ab19870), LXRα (1:1000, Abcam, catalog number: ab106464) or LXRβ (1:1000, Abcam, ab28479) overnight at 4 °C. The membranes were washed with TBS-Tween-20 for 3 times and incubated with secondary antibody horseradish peroxidase-conjugated rabbit anti-goat, goat anti-mouse or goat anti-rabbit IgG for 2 h at room temperature. The blots were developed with enhanced chemiluminescence (Clarity™ Western ECL Substrate, Bio-Rad) and detected by a Tanon 5200 imager (Tanon Science & Technology Co., Ltd., Shanghai, China). The blots were analyzed by Tanon MP Software (Tanon Science & Technology Co., Ltd. Shanghai, China). Intensities of the blots were quantified and normalized against a loading control (β-actin), by an investigator blinded to the experimental conditions.

2.5. Immunohistochemistry

Immunohistochemistry was performed as described according to our previous studies (Wei et al. 2013; Ying et al., 2014; Song et al., 2018). Briefly, rats that have received LTP recording were perfused with saline, through the ascending aorta, followed by 4% paraformaldehyde in 0.1 M phosphate buffer. The lumbar spinal cord segments were carefully removed and postfixed in the same fixative for 2–4 h, after witch the samples were placed in 30% sucrose and kept in 4 °C for 48 h. Transverse free-floating spinal sections (25 μm) were cut by a cryostat (Leica CM 1900; Heidelberg, Germany), during which no randomization methods were employed and the spinal cord sections were arbitrarily chosen for immunofluorescence staining.

All the selected sections were incubated in blocking buffer (3% donkey serum in 0.3% Triton X-100) for 1 h at room temperature and then incubated with primary antibodies, including rabbit anti-SIRT1 antibody (1: 300; Cell signaling Technology), rabbit anti-ac-p65 antibody rabbit anti-LXRα (1:200, Abcam) or rabbit anti-LXRβ (1:300, Abcam) antibody, from the same batches that were used in the western blotting analysis, over 2 nights at 4 °C. The sections were then incubated for 1 h at room temperature with Cy3 - conjugated secondary antibodies (1:500, Jackson ImmunoResearch, West Grove, PA, USA). For the negative control sections, the above procedures were followed except that no primary antibodies were added.

For double immunofluorescence staining of LXRα, LXRβ, or SIRT1 with tissue markers, primary antibodies from the same batches as in the above were incubated together with antibody for mouse monoclonal neuronal-specific nuclear protein (NeuN, neuronal marker, Millipore, USA), or glial fibrillary acidic protein (GFAP, 1:500, astrocyte marker, Cell Signaling Technology), or goat polyclonal anti-ionized calcium-binding adaptor molecule 1 (Iba1, 1:500, microglia marker, Abcam) for 2 nights at 4 °C. For double immunofluorescence staining of LXRα or LXRβ with SIRT1, after the primary antibodies (LXRs antibodies were as in the above, mouse anti-SIRT1 antibody ab110304 from abcam) incubation, the above spinal sections were treated with a mixture of cy3-conjugated and FITC-conjugated secondary antibodies (Jackson ImmunoResearch) for 1 h at room temperature.

The sections were then examined with a Leica (Leica, Wetzlar, Germany) fluorescence microscope or with LSM 780 confocal microscope (Zeiss, Germany).

2.6. RNA extraction and real-time quantitative polymerase chain reaction (RT-qPCR)

Total RNA from the lumbar spinal cord was extracted by a TRIzol reagent (Invitrogen, USA). The reverse transcription was performed using PrimeScript RT Master Mix (Takara, China). Real-time qPCR was processed with SYBR Premix Ex Taq^{TM}II (Takara). The relative ratio of mRNA expression was quantified through the $2-\Delta\Delta CT$ method. The primer sequences were as the following, TNFα forward: TTCCAATGG GCTTTCGGAAC, TNFα Reverse: AGACATCTTCAGCAGCCTTGTGAG, LXRα forward: CAACCCTGGGAGTGAGAGCA, LXRα Reverse: GCAGT TCATTCATGGATCTGGAG, LXRβ forward: CCTACAGCAAGGACGACTT CCAC, LXRβ Reverse: GCAAGGCATACTCTGCATCGTCTA, SIRT1 forward: ACCTCCTCATTGTTATTGGGTCTTC, SIRT1 Reverse: GGCATACT CGCCACCTAACC.

2.7. Quantification and statistics

The amplitude of C-fiber evoked field potentials was determined offline by parameter extraction, which was implemented by ADC-42 (Fig. 1 top). In each experiment, c-fiber evoked responses to five consecutive test stimuli were averaged. The mean amplitudes of C-fiber responses before drug or vehicle application served as baseline. All data were expressed as means ± SEM. Statistical tests were performed with SPSS 16.0 (SPSS Inc., Chicago, IL, USA) by an investigator that did know the experimental conditions. It was considered there is a statistical significance if $p < 0.05$ was. The effects of SMIR and various drugs on C-fiber evoked field potentials were analyzed using repeated measures ANOVA with Tukey's post hoc test when compared within the same group, or nonparametric tests with Mann-Whitney-U-test when compared between groups. Western blotting and real-time qPCR data were analyzed by one-way ANOVA followed by Tukey's post hoc test. The normality of the data was firstly checked by Shapiro-Wilk test. If $P > 0.05$, the data were considered normally distributed and therefore AN OVA was used. Otherwise Mann-Whitney tests were used.

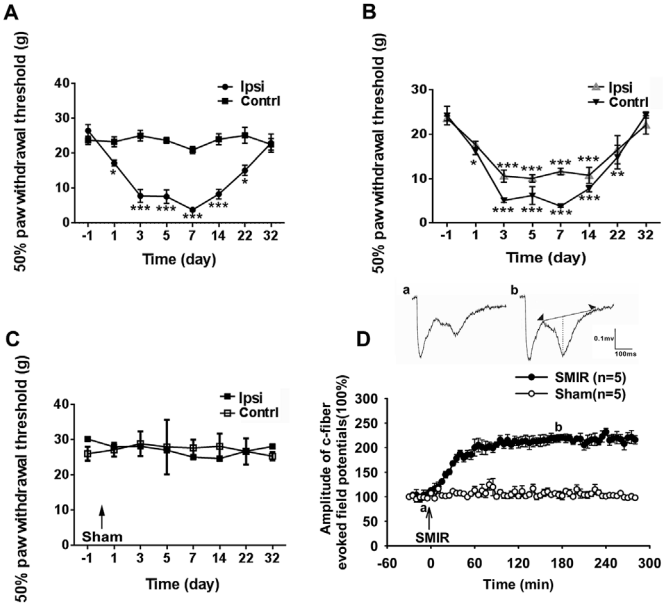

Fig. 1. SMIR induced mechanical allodynnia and LTP of C-fiber-evoked field potentials in spinal dorsal horn
A, In 5 rats, SMIR induced mechanical allodynia in the ipsilatral but not contralateral hind paw. B, In another 5 rats, SMIR induced mechanical allodynia in bilateral hind paw. C, Sham operation did not induce changes in bilateral hind paw. D, In one group of rats (closed circle, n = 5), after stable recording of C-fiber evoked field potentials for 30 min, the retraction of the skin and superficial muscle of the thigh potentiated the C-fiber evoked response in the spinal dorsal horn gradually. In another group of animals (open circle, n = 5), which received skin and muscle incision but no retraction, the C-fiber evoked response remained intact. Representative traces of field potentials, which were recorded before (a) and after (b) SMIR from one animal, are shown at the top. In A and B, *P < 0.05, *P < 0.01, ***P < 0.001 compared with sham group.

3. Results

3.1. SMIR induced mechanical allodynia and long term potentiation at C-fiber synapses in spinal dorsal horn

As shown in Fig. 1A, in one group of rats (n = 5), the 50% paw withdrawal threshold on the ipsilateral to the SMIR surgery was already significantly decreased on day 1 ($p < 0.05$ compared with day −1), which decreased further on day 3 ($p < 0.01$ compared with day −1), and returned to the baseline level on day 32. The 50% paw withdrawal threshold in the contralateral side did not decrease at all the time points that we tested, indicating that unilateral mechanical allodynia developed in these rats. In another group of rats, decrease in 50% paw withdrawal threshold was observed on day 1 and 3 in the ipsilateral and contralateral paw, respectively (Fig. 1B, n = 5), indicating that bilateral mechanical allodynia developed in these rats. The pain behaviors on the contralateral side were much weaker and lasted much shorter than those on the ipsilateral side. Sham operation, during which rats

received skin and muscle incision but no retraction did not affect the 50% paw withdrawal threshold (Fig. 1C).

After having demonstrated that SMIR induced pain behaviors, we next investigated whether SMIR induced LTP of C-fiber evoked field potential, as spinal LTP is a marker of central sensitization that underlies some forms of hyperalgesia. To do so, an incision (7–10 mm long) was firstly made in the superficial muscle layer of the thigh and a micro dissecting retractor was implanted into the muscle but not dissected. After stable recording of C-fiber evoked field potentials for 30 min, the skin and superficial muscle of the thigh was carefully retracted by 2 cm without stopping the recording. The retraction persisted for 1 h. As shown in Fig. 1D, SMIR potentiated the C-fiber evoked responses gradually. 10 min after the retraction, the amplitude of C-fiber evoked field potentials was already significantly increased (123.91 ± 3.64% at 10 min, $P < 0.01$ compared to baseline), which then gradually increased to a stable plateau (232.05 ± 7.35% of baseline 4 h after the beginning of the retraction, $P < 0.001$), and lasted at least 280 min.

3.2. TNFα was increased following SMIR and that spinal application of TNFα neutralization antibody prevented SMIR-induced LTP

Studies from our group have shown that TNFα in the spinal cord plays a critical role in LTP induction following high frequency stimulation (Zhong et al., 2010) or spinal application of remifentanil (Yang et al., 2018). To test whether spinal TNFα contributed to SMIR-induced spinal LTP, firstly we detected the mRNA and protein level of TNFα in the ipsilateral lumbar spinal dorsal horn by qPCR and Western blotting, and then tested whether spinal application of TNFα neutralizing antibody could block the induction of LTP following SMIR. As shown in Fig. 2A, we found that compared to the sham group, TNFα mRNA was gradually increased 60 and 240 min after SMIR ($P < 0.001$). TNFα protein was also gradually increased following SMIR (Fig. 2B, to 153.24 ± 5.96% of sham at 30 min, $P < 0.01$; to 183.60 ± 8.1%5 of sham at 240 min, $P < 0.001$). Spinal application of anti-rat TNF-α neutralization antibody (0.6 μg/ml, in 200 μl volume) 30 min before SMIR completely abolished the induction of LTP following SMIR, whereas spinal application of PBS (0.01 M, 200 μl volume), which was used to dissolve TNFα neutralization antibody, had no effect on the induction of LTP (Fig. 2C).

3.3. Expression of acetylated NF-κB p65 (ac-NF-κB p65) was increased following SMIR and spinal application NF-κB inhibitor PDTC prevented SMIR-induced LTP

Ac-NF-κB p65 is a central proinflammatory mediator and can be activated under various stimulus, here we investigated whether SMIR affected the acetylation of p65 (on lysine 310) by Western blotting. As shown in Fig. 2D, the protein level of ac-p65 in lumbar spinal dorsal horn was gradually increased following SMIR (157.86 ± 8.91% of control at 30 min, $P < 0.001$, to 215.85 ± 9.52 of control at 240 min, $P < 0.001$). Immunohistochemistry also showed that there were more ac-p65 positive signals in the spinal dorsal horn the SMIR rats than that in the sham group at 240 min (Fig. 2E). Spinal application of NF-κB inhibitor PDTC (10 pM in 200 μl volume) but not saline (200 μl volume), 30 min before SMIR, also abolished the induction of LTP (Fig. 2F).

3.4. Expression of SIRT1 was decreased following SMIR and activation of SIRT1 by SRT1720 prevented SMIR-induced LTP

SIRT1 can directly deacetylate the ly310 residue of the NF-κB p65 subunit. Next we observed whether SMIR affected the mRNA and protein expression of SIRT1 at different time points. As shown in Fig. 3A, compared with sham group, the SIRT1 mRNA began to decrease since 15 min ($p < 0.05$), and the decrease reached its maximum level at 60 min after SMIR ($p < 0.001$). Western blotting showed that SIRT1 protein decreased since 30 min (82.96 ± 3.84 of baseline, $p < 0.05$) after SMIR, and decreased further at 60 min (79.44 ± 3.77, $p < 0.01$). At 4 h after the retraction, the expression of SIRT1 decreased to only 57.81 ± 2.67% of sham group. Immunofluroscience staining confirmed the results of western blotting at 240 min (Fig. 3C–D). Double Immunofluroscience further showed that SIRT1 was located exclusively in neurons (Fig. 3E and H), but not in Iba1 labeled microglia (Fig. 3F and I) or in GFAP labeled astrocytes (Fig. 3G and J), either in SMIR (4 h) rats or in sham operated rats. Spinal application of SIRT1 agonist SRT1720 (10 pM in 200 μl volume) but not DMSO, 30 min before SMIR abolished the induction of LTP (Fig. 4), as 4 h after SRT1720

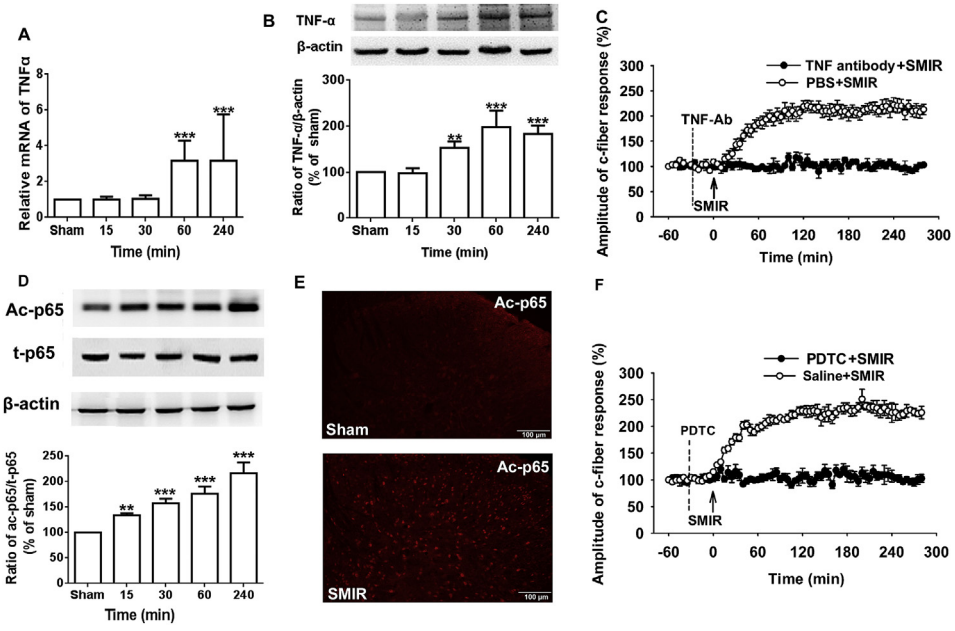

Fig. 2. SMIR increased expression of TNFα and Ac-NF-Kb p65 in the lumbar spinal dorsal horn, and spinal application of TNFα neutralization antibody or NF-κB inhibitor prevented SMIR-induced spinal LTP

A, Compared with the sham rats, expression of TNFα mRNA was increased in the lumbar spinal dorsal horn since 60 min after SMIR, and the increase persisted till 4 h after SMIR. B, Compared with the sham rats, expression of TNFα protein was increased in the lumbar spinal dorsal horn since 30 min after SMIR, and the upregulation lasted at least 4 h. C, Application of TNFα neutralization antibody (0.6 μg/ml, in 200 μl volume) but not PBS (0.01 M, 200 μl volume) to the spinal cord, 30 min before SMIR completely abolished SMIR-induced spinal LTP. D, Compared with the sham rats, increased expression of ac-NF-Kb p65 was observed by Western blotting in the lumbar spinal dorsal horn since 15 min after the surgery in SMIR rats, which lasted at least 4 h. E, Immunhistochemistry showed that expression of ac-NF-Kb p65 was increased in the lumbar spinal dorsal horn at 240 min after SMIR, compared to the sham group. F, Application of PDTC (10 pM in 200 μl volume) but not saline (200 μl volume) to the spinal cord, 30 min before SMIR prevented the induction of LTP. In A, B and D $^{**}P < 0.01$, $^{***}P < 0.001$ compared with sham group. n = 5/group.

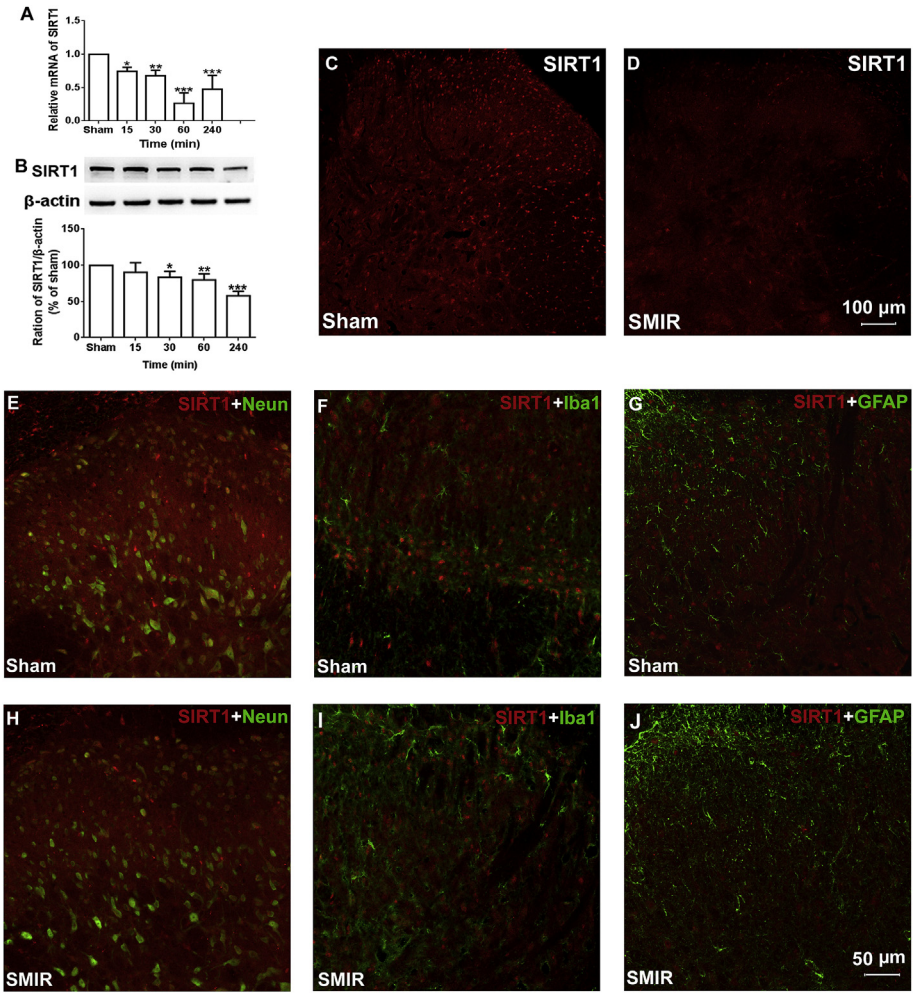

Fig. 3. Expression of SIRT1 in neurons was reduced following SMIR

A, The expression of SIRT1 mRNA was decreased since 15 min after SMIR, and lasted at least 240 min. B, Western blotting showed that the protein expression of SIRT1 was significantly decreased at 30 min, and decreased further at 60 min following SMIR. The protein reduction lasted at least 4 h. C-D, Representative experiments show the changes of SIRT1-IR in the ipsilateral lumbar spinal dorsal horn 4 h after sham (C) or SMIR (D) surgery E-J, Double immunofluroscience staining showed that SIRT1 was expressed exclusively in neurons, but not in microglia or astrocytes, in either sham (E-G) or SMIR (H-J) rats. Scale bar (C-D) 100 μm (B-I) 50 μm. For A-B, *P < 0.05, **P < 0.01, ***P < 0.001 compared with sham group. n = 5/group.

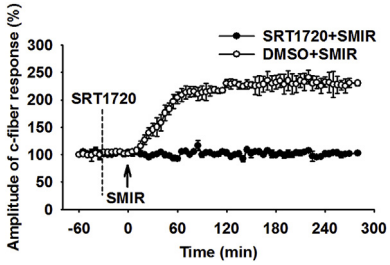

Fig. 4. Spinal application of SIRT1 agonist SRT1720 but not DMSO prevented the induction of LTP

Application of SRT1720
(10 pM in 200 μl volume) onto the spinal dorsal horn, 30 min before SMIR completely abolished the induction of LTP following SMIR, whereas application of DMSO (200 μl) had no effect. n = 5/group.

administration to the spinal cord, the c-fiber evoked response was 102.84 ± 2.18 of baseline, whereas after DMSO administration, the c-fiber evoked response was 230.43 ± 5.52 of baseline.

3.5. Expression of liver X receptors was increased in neurons following SMIR

Compared with the sham group (Fig. 5A), qPCR and Western blot analysis demonstrated that the mRNA and protein level of LXRα and LXRβ in the ipsilateral lumbar spinal dorsal horn was increased significantly following SMIR (Fig. 5A–D), with the increase of LXRα lasted longer than LXRβ. Immunohistochemistry showed that the expression of LXRα was mainly in neurons (Fig. 5G and K), but not in microglia (Fig. 5H and L) or astrocytes (Fig. 5I and M), both in the sham operated or SMIR rats, at 240 min after SMIR. Similarly, the expression of LXRβ was located exclusively in neurons (Fig. 5P–T), but not in microglia (Fig. 5Q and U) or astrocytes (Fig. 5R and V) at 60 min after SMIR. No signals were detected in the negative control group (Fig. 5E and N), when no primary antibodies were added.

3.6. Spinal application of liver x receptors agonist T0901317 prevented LTP induced by SMIR

Spinal application of T0901317 (0.25 μM in 200 μl volume) but not DMSO, 30 min before SMIR also abolished the induction of LTP (99.08 ± 2.76% at 240 min for T09 group, P > 0.05 compared to baseline, P < 0.05 compared to DMSO group). Application of 0.05 μM T0901317 (in 200 μl volume) had no effect on the induction of LTP following SMIR (238.02 ± 9.87% at 240 min, P < 0.05 compared to baseline, Fig. 6).

3.7. Spinal application of T0901317 upregulated the expression of SIRT1, which was colocalized with LXRs, and decreased the expression of ac-NF-kB p65 and TNFα in SMIR rats

Further experiments showed that SIRT1 was colocalized with either LXRα (Fig. 7A–C) or LXRβ (Fig. 7D–F), with SIRT1 and LXRα at almost the same location and LXRβ circling SIRT1. In order to further elucidate the role of SIRT1 in LXRs agonist-elicited inhibitory effect on SMIR-induced LTP, effects of T0901317 on the expression of SIRT1 and the

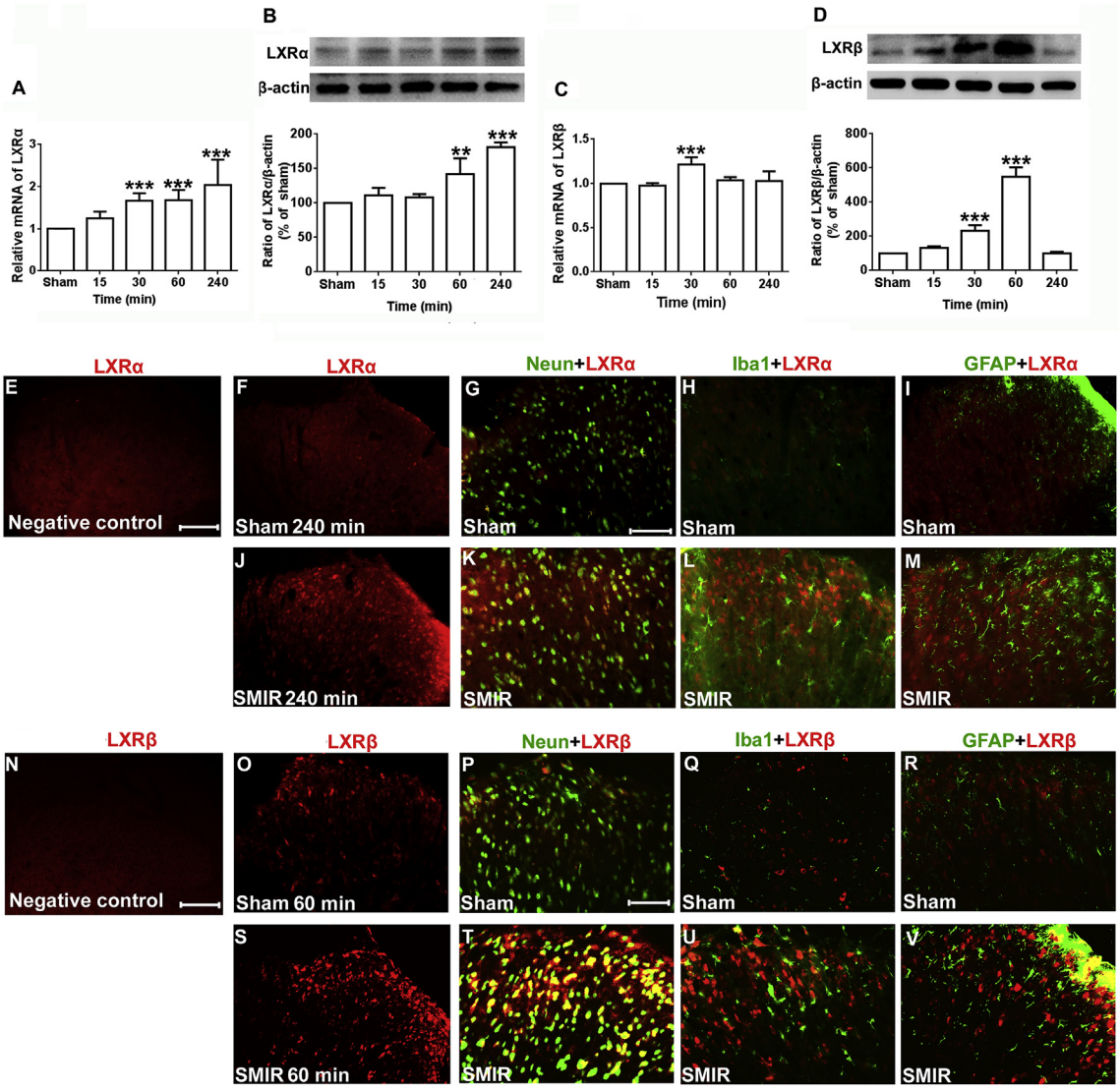

Fig. 5. The expression of LXRs in neurons was increased following SMIR

A, LXRα mRNA was increased 30 min after SMIR, and lasted at least 240 min ***P < 0.001 compared with sham group (n = 5/group). ***P < 0.001 compared with sham group. B, The band shows the protein level of LXRα in the 5 different groups (n = 4/group), **P < 0.01, ***P < 0.001 compared with sham group., C-D, mRNA and protein level of LXRβ was transiently increased following SMIR. ***P < 0.001 compared with sham group. E and N, No signals were detected by immunohistochemistry in the negative control group. F-M, Immunohistochemistry showed the increased expression of LXRα was located only in neurons in both sham operated and SMIR (4 h post-injury) rats. O-V, LXRβ was located only in neurons, but not in microglia or astrocytes, in both sham operated and SMIR (1 h post-injury) rats. Scale bar (E, F, J, N, Q and S): 100 μm; The left: 50 μm n = 4–5/group.

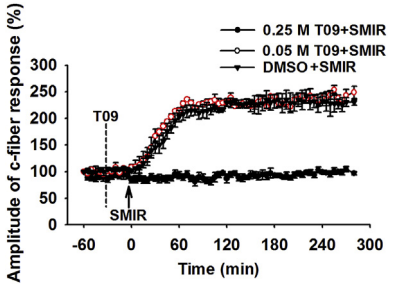

Fig. 6. Spinal application of LXRs agonist T0901317 but not DMSO prevented the induction of LTP.

Application of T0901317 (0.25 μM in 200 μl volume) onto the spinal dorsal horn, 30 min before SMIR, completely abolished the induction of LTP following SMIR, whereas application of T0901317 (0.05 μM in 200 μl volume) or DMSO (200 μl) had no effect (n = 5/group).

subsequent NF-kB/TNFα pathway was evaluated. Western blotting showed that in those SMIR rats that received spinal application of T0901317, the protein level of SIRT1 was significantly increased 4 h after the drug application, whereas in these rats that received DMSO administration, the expression of SIRT1 was still deceased compared to the sham group (Fig. 7G). Further experiments showed that T0901317 but not DMSO decreased the expression of ac-NF-κB p65 and TNFα (Fig. 7H–I) in SMIR rats, 4 h after the drugs application.

3.8. SIRT1 antagonist EX-527 abolished the effect of T0901317 on SMIR-induced LTP, and on expression of ac-NF-kB p65 and TNFα

We further investigated whether T0901317 really effected via SIRT1. Electrophysiology recording showed that pretreatment with EX-527, a SIRT1 antagonist, blocked the inhibitory effect of T0901317 on LTP induction, as in these rats that received EX-527 treatment before T0901317, the c-fiber evoked response was still potentiated (208.53 ± 11.05 of baseline at 4 h after SMIR, P < 0.05, Fig. 8A),

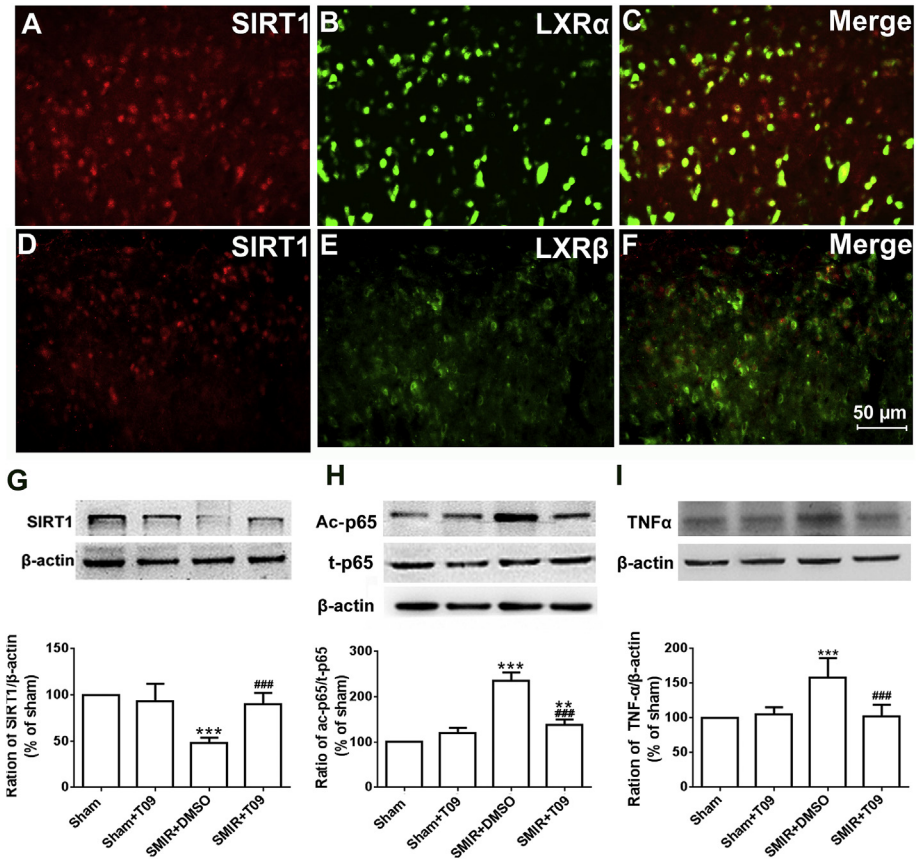

Fig. 7. SIRT1 was colocalized with LXRs and spinal application of T0901317 induced SIRT1 expression, decreased the expression of ac-NF-kB p65 and TNFα in SMIR rats.

A-F, Representative pictures show that SIRT1 was largely colocalized with LXRα (A-C) or LXRβ (D-F). G, Spinal application of T0901317 but not DMSO significantly increased the expression of SIRT1, 4 h after the drug application. H-I, Spinal application of T0901317 but not DMSO decreased the expression of Ac-NF-κB p65 (H) and TNFα (I) in SMIR rats, 4 h after the drug application (n = 5/group). ***p < 0.001 compared with sham group, ###p < 0.001 compared with SMIR + DMSO group.

whereas in these rats that received saline treatment before T0901317, the c-fiber response was not increased (102.76 ± 4.08% at 4 h of baseline, P > 0.05 Fig. 8A). Moreover, EX-527 pretreatment abolished the inhibitory effect of T0901317 on expression of ac-NF-kB (Fig. 8B) and TNFα (Figs. 8C) and 4 h after T0901317 application.

4. Discussion

The present study revealed that SMIR surgery induced LTP of c-fiber evoked field potentials. During LTP induction, the expression of TNFα and ac-NF-κB p65 was gradually increased in the lumbar spinal dorsal horn, while spinal application with either TNFα neutralization antibody or NF-κB inhibitor PDTC completely prevented the induction of LTP. Moreover, the mRNA and protein expression of SIRT1 in the lumbar spinal dorsal horn was decreased and activation of SIRT1 also prevented the induction of LTP. Importantly, mRNA and protein level of LXRs, was enhanced in the lumbar spinal dorsal horn, while spinal application of LXRs agonist also prevented the induction of LTP. Further experiments showed that T0901317 enhanced SIRT1 protein expression, which was colocalized with LXRs. T0901317 also decreased the NF-κB acetylation and TNFα protein expression. The effect of T0901317 on LTP, on expression of ac-NF-κB p65 and TNFα was blocked by SIRT1 antagonist. These results indicated that NF-κb/TNFα pathway activation, followed by decreased SIRT1 expression, contributed to the induction of LTP after SMIR, and that activation of LXRs prevented LTP by inhibiting NF-κB/TNFα pathway via activating SIRT1.

4.1. The mechanisms that mediate LTP induction following SMIR

Studies from our group have shown that spinal application of ATP (Gong et al., 2009), BDNF (Zhou et al., 2008) or remifentanil (Yang et al., 2018) can induce spinal LTP at C-fiber synapses in the absence of conditioning activation of primary afferents. In the present study, we further showed that skin incision and muscle retraction of the thigh, which resulted in neither saphenous nerve demyelination or injury (Flatters, 2008; Ying et al., 2014), induced spinal LTP at C-fiber synapses. The electrical recording was performed at L5 spinal cord, which receives projection predominantly from the sciatic nerve, whereas the retracted sapherous nerve is known to have inputs into the spinal cord at L3 and L4 level (Bajrovic and Sketelj, 1998). Therefore we believed the LTP induced by SMIR here is a kind of heterosynaptic LTP, which was independent of C-fiber inputs. In the present study, we further found that TNFα expression was significantly increased from 30 min after SMIR, and that TNFα neutralization by its antibody prevented the induction of LTP. Thus it is high possible that during the retraction, cytokines such as TNFα are released into the L3 and L4 spinal cord segments, and then diffuse into the L5 segment to sensitize the neurons there to induce spinal LTP. It is well known that microglia, when being activated, can release bioactive substances including TNFα and ATP. Our previous study has shown that spinal microglia is activated following SMIR (Ying et al., 2014). Mounting evidence has demonstrated that microglia is activated during HFS, remifentani, BzATP, or BDNF-induced LTP (Chu et al., 2012; Yang et al., 2018; Kronschlager et al., 2016; Zhou et al., 2011). Therefore it is very likely that microglia activation, by whatever method, is a common reason for LTP induction, no matter it is homosynaptic or heterosynaptic.

Previously it has been reported that upregulation of reactive oxygen species (ROS) can increases the excitability of wide dynamic range (WDR) neurons in the spinal dorsal horn (Kim et al., 2015). Prolonged retraction of the thigh during SMIR surgery may render the soft tissue anoxic, impacts the mitochondria and result in energy metabolism imbalance, which may then induce a large amount of ROS release. It has been reported that ROS produced following oxidative stress down-regulates the expression and the activity of SIRT1, by directly oxidizing the cystine residues of SIRT1 protein and thus inactivate SIRT1 activity,

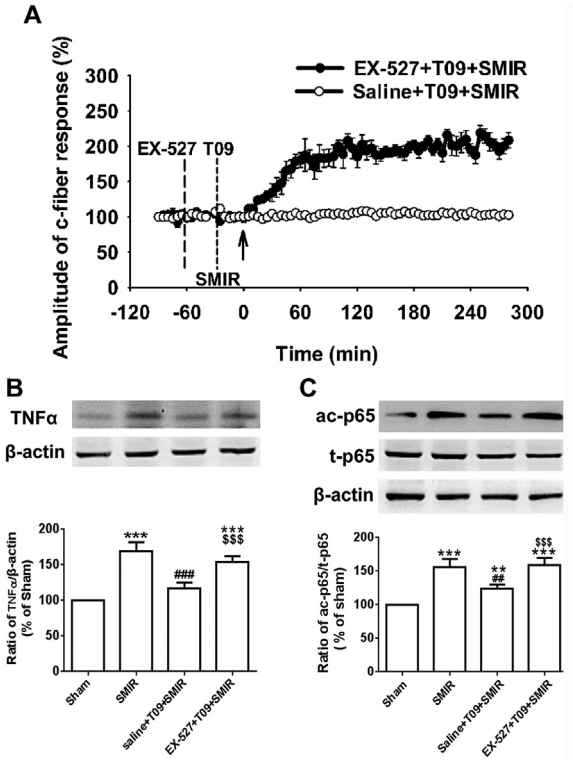

Fig. 8. SIRT1 antagonist EX-527 abolished the effect of T0901317 on SMIR-induced LTP, on expression of ac-NF-kB and TNFα. A, Spinal application of EX-527 but not saline, 30
min before T0901317, blocked the inhibitory effect of T0901317 on c-fiber evoked field potentials (n =
5/group). B-C, Western blotting showed that EX-527 pretreatment abolished the inhibitory effect of T0901317 on expression of TNFα (B) and ac-NF-κB p65 (C), 4 h after T0901317 application (n = 5/group). ***P < 0.001 compared with sham group; ###P < 0.001 compared with SMIR group. $$$ P < 0.001 compared with saline + T09 + SMIR group.

and then lead to the protein degradation in proteasomes (Rajendrasozhan et al., 2008; Caito et al., 2010). Consistently here we found that accompanied by LTP development, SMIR decreased SIRT1 expression in neurons, whereas activation of SIRT1 prevented LTP induction following SMIR. A line of previous study has shown that in diabetic neuropathic pain rats, SIRT1 expression in the spinal cord was downregulated, and that intrathecal injection of SIRT1 agonist attenuates pain behaviors (Zhou et al., 2017). In addition, specific lack of SIRT1 induced pain behaviors, dietary obesity and type 2 diabetes in normal rats (Zhou et al., 2017; Ramadori et al., 2011), whereas SIRT1 overexpression provided protection against metabolic imbalance (Ramadori et al., 2011). These studies, together with our results, highly suggest that following SMIR, the bioactive substances, such as ROS are released and diffused to the spinal cord and then downregulate or inactivate SIRT1 there. Previously it has been reported that SIRT1 can suppress the transcription of the NF-κB-dependent gene by directly interact with and deacetylate the ly310 residue of the RelA/p65 subunit (Yeung et al., 2004; Kauppinen et al., 2013). It has also been shown that SIRT1 activation can result in activation of AMP-activated protein kinase (AMPK), Peroxisome-proliferator-activated receptor alpha (PPARα) and PPAR gamma co-activator 1 alpha (PGC-1α) (Kauppinen et al., 2013), which play an important role in energy metabolism. Thus besides direct inhibition on NF-κb pathway, SIRT1 activation can inhibit NF-κB signaling indirectly by activating AMPK, PPARα and PGC-1α to rebalance the energy metabolism. Moreover, Lys 310 deacetylation in the p65 protein exposed it to methylation at Lys 314 and Lys 315, which enhanced its ubiquitination and degradation (Yang et al., 2010). So SIRT1 has a significant role in the termination of the inflammatory response driven by NF-κB. The decreased SIRT1 activity following SMIR may result in NF-κB p65 acetylation, translocation and activation, and then induce subsequent expression of numerous genes, such as TNFα. The increased TNFα then potentiate the synaptic transmission at c-fiber synapses by increasing AMPAR in the membrane, by increasing AMPA receptors and decreasing expression of GABAA receptors in the cell surface (Stellwagen et al., 2005).

4.2. The mechanisms that activation of LXRs inhibits SMIR-induced LTP

LXRs are nuclear receptors activated by oxysterols that play critical roles in regulating cholesterol, fatty acid metabolism and lipid metabolism (Wang and Tontonoz, 2018). LXRα and LXRβ share 80% homology in their DNA and ligand binding domains (Zhao and Dahlman-Wright, 2010). It has been reported that enhanced LXR activity is protective against diabetes-induced retinal vascular damage and that activation of LXRs in dorsal root ganglia protect from Endoplasmic Reticulum stress and mechanical allodynia in western diet -fed mice (Gavini et al., 2018). Conversely, knockout of LXRs caused retinal vascular damage or lipid accumulation in macrophages, splenomegaly, and increased atherosclerosis (Schuster et al., 2002; Tangirala et al., 2002). Furthermore, the loss of LXRα/β in Nav1.8 positive neurons in nodose ganglia enhances mitochondrial respiration, through which a large amount of ROS can be produced, in skeletal muscle (Mansuy-Aubert et al., 2015). In the present study, we found that the expression of LXRα and LXRβ was increased in the ipsilateral lumbar spinal dorsal horn after SMIR and that spinal application of LXR agonist T0901317 prevented LTP induction. These results suggest that enhancement of LXRs is a protective factor to dampen LTP development following SMIR, however, LXRs expression by itself may be not enough to completely dampen the induction of LTP, possibly because the endogenous ligands were not enough. When LXRs agonist was supplemented to the spinal cord, the dampening factor can be strengthened, and spinal LTP induction could be prevented. In the present study, we further found SIRT1 was colocalized with LXRs and that 4 h after T0901317 application to the spinal cord, when c-fiber evoked field potentials was already deceased, the expression of SIRT1 in lumbar spinal cord was increased, whereas the expression of ac-NF-κB and TNFα was decreased. Moreover, pretreatment with SIRT1 antagonist EX-527 completely abolished the inhibiting effect of T0901317 on ac-NF-κB and TNFα. LXRs and SIRT1 are both key metabolic regulators that have been shown to be located in nuclear, and LXRs have not been shown to function as a ligand-dependent transcriptional repressor. These results indicated that LXRs function via increasing SIRT1 expression, which then inhibit NF-κb mediated cytokine release. In primary macrophages, deficiency of SIRT1 decreases the induction of the LXRs target gene ABCA1, impairing cholesterol export, whereas activation of SIRT1 enhanced LXRα activity, and expression of ABCA1 and ABCG1 (Li et al., 2007). These studies, together with our results, indicated that the ligand activation of LXRs prevented LTP induction by activating SIRT1, which then inhibit NF-κB/TNFα directly or indirectly following SMIR. Moreover, there seems to be a positive feedback between LXRs and SIRT1 activation. Activation of SIRT1, followed by LXR deacetylation at a single conserved lysine (K432 in LXRα and K433 in LXRβ) adjacent to the ligand-regulated activation domain, leads to LXRs activation and inhibition of NF-κB activity (Li et al., 2007; Zeng et al., 2013). This positive feedback, that is, activation of LXRs increase SIRT1 expression, which then deacetylates LXRs and further activate it, may helps to interrupt the series of events following SMIR to prevent LTP.

In conclusion, our current work demonstrated a favorable role of the LXR agonist in SMIR-induced LTP, possibly associated with SIRT1 activation and subsequent NF-κB/TNFα pathway inhibition. Our study may guide prospective clinical trials to assess the latent preventive effects of the LXR agonist on CPSP.

Conflicts of interest

The authors declare that they have no conflicts of interest.

Acknowledgments

This work was supported by grants from the National Natural Science Foundation (Beijing, People's Republic of China. Nos. 81870969 and 81471250); Nature Science Foundation of Guangdong Province of China (Guangzhou, People's Republic of China. No.s 2017A030313132 and 2017A030313839); Scientific Research Foundation of Guangdong Province of China (Guangzhou, People's Republic of China. No.s. 2013B02200001 and 2016A020215035).

Appendix A. Supplementary data

Supplementary data to this article can be found online at https://doi.org/10.1016/j.neuint.2019.04.002.

References

Bagul, P.K., Deepthi, N., Sultana, R., Banerjee, S.K., 2015. Resveratrol ameliorates cardiac oxidative stress in diabetes through deacetylation of NFkB-p65 and histone 3. J. Nutr. Biochem. 26, 1298–1307.

Bajrovic, F., Sketelj, J., 1998. Extent of nociceptive dermatomes in adult rats is not primarily maintained by axonal competition. Exp. Neurol. 150, 115–121.

Bao, X., Cai, Y., Wang, Y., Zhao, J., He, X., Yu, D., Huang, J., Jing, S., Du, Z., Yang, T., Warner, M., Gustafsson, J.A., Fan, X., 2017. Liver X receptor beta is involved in formalin-induced spontaneous pain. Mol. Neurobiol. 54, 1467–1481.

Baud, V., Collares, D., 2016. Post-translational modifications of RelB NF-kappaB subunit and associated functions. Cells 5 (5).

Cermenati, G., Abbiati, F., Cermenati, S., Brioschi, E., Volonterio, A., Cavaletti, G., Saez, E., De Fabiani, E., Crestani, M., Garcia-Segura, L.M., Melcangi, R.C., Caruso, D., Mitro, N., 2012. Diabetes-induced myelin abnormalities are associated with an altered lipid pattern: protective effects of LXR activation. J. Lipid Res. 53, 300–310.

Caito, S., Hwang, J.W., Chung, S., Yao, H., Sundar, I.K., Rahman, I., 2010. PARP-1 inhibition does not restore oxidant-mediated reduction in SIRT1 activity. Biochem. Biophys. Res. Commun. 392, 264–270.

Chen, K., Fan, J., Luo, Z.F., Yang, Y., Xin, W.J., Liu, C.C., 2018. Reduction of SIRT1 epigenetically upregulates NALP1 expression and contributes to neuropathic pain induced by chemotherapeutic drug bortezomib. J. Neuroinflammation 15, 292.

Chu, Y.X., Zhang, Y., Zhang, Y.Q., Zhao, Z.Q., 2010. Involvement of microglial P2X7 receptors and downstream signaling pathways in long-term potentiation of spinal nociceptive responses. Brain Behav. Immun. 24, 1176–1189.

Chu, Y.X., Zhang, Y.Q., Zhao, Z.Q., 2012. Involvement of microglia and interleukin-18 in the induction of long-term potentiation of spinal nociceptive responses induced by tetanic sciatic stimulation. Neurosci. Bull. 28, 49–60.

Dai, B., Lei, C., Lin, R., Tao, L., Bin, Y., Peng, H., Lei, B., 2017. Activation of liver X receptor alpha protects amyloid beta 1-40 induced inflammatory and senescent responses in human retinal pigment epithelial cells. Inflamm. Res. 66, 523–534.

Flatters, S.J., 2008. Characterization of a model of persistent postoperative pain evoked by skin/muscle incision and retraction (SMIR). Pain 135, 119–130.

Gavini, C.K., Bookout, A.L., Bonomo, R., Gautron, L., Lee, S., Mansuy-Aubert, V., 2018. Liver X receptors protect dorsal root ganglia from obesity-induced endoplasmic reticulum stress and mechanical allodynia. Cell Rep. 25, 271–277.

Gong, Q.J., Li, Y.Y., Xin, W.J., Zang, Y., Ren, W.J., Wei, X.H., Li, Y.Y., Zhang, T., Liu, X.G., 2009. ATP induces long-term potentiation of C-fiber-evoked field potentials in spinal dorsal horn: the roles of P2X4 receptors and p38 MAPK in microglia. Glia 57, 583–591.

Han, D., Li, X., Li, S., Su, T., Fan, L., Fan, W.S., Qiao, H.Y., Chen, J.W., Fan, M.M., Li, X.J., Wang, Y.B., Ma, S., Qiu, Y., Tian, Z.H., Cao, F., 2017. Reduced silent information regulator 1 signaling exacerbates sepsis-induced myocardial injury and mitigates the protective effect of a liver X receptor agonist. Free Radic. Biol. Med. 113, 291–303.

Kauppinen, A., Suuronen, T., Ojala, J., Kaarniranta, K., Salminen, A., 2013. Antagonistic crosstalk between NF-kappaB and SIRT1 in the regulation of inflammation and metabolic disorders. Cell. Signal. 25, 1939–1948.

Kim, H.Y., Lee, I., Chun, S.W., Kim, H.K., 2015. Reactive oxygen species donors increase the responsiveness of dorsal horn neurons and induce mechanical hyperalgesia in rats. Neural Plast. 293423 2015.

Klein, T., Magerl, W., Nickel, U., Hopf, H.C., Sandkuhler, J., Treede, R.D., 2007. Effects of the NMDA-receptor antagonist ketamine on perceptual correlates of long-term potentiation within the nociceptive system. Neuropharmacology 52, 655–661.

Klein, T., Magerl, W., Treede, R.D., 2006. Perceptual correlate of nociceptive long-term potentiation (LTP) in humans shares the time course of early-LTP. J. Neurophysiol. 96, 3551–3555.

Kronschlager, M.T., Drdla-Schutting, R., Gassner, M., Honsek, S.D., Teuchmann, H.L., Sandkuhler, J., 2016. Gliogenic LTP spreads widely in nociceptive pathways. Science 354, 1144–1148.

Liu, X.G., Zhou, L.J., 2015. Long-term potentiation at spinal C-fiber synapses: a target for pathological pain. Curr. Pharmaceut. Des. 21, 895–905.

Lv, C., Hu, H.Y., Zhao, L., Zheng, H., Luo, X.Z., Zhang, J., 2015. Intrathecal SRT1720, a SIRT1 agonist, exerts anti-hyperalgesic and anti-inflammatory effects on chronic constriction injury-induced neuropathic pain in rats. Int. J. Clin. Exp. Med. 8, 7152–7159.

Mansuy-Aubert, V., Gautron, L., Lee, S., Bookout, A.L., Kusminski, C., Sun, K., Zhang, Y., Scherer, P.E., Mangelsdorf, D.J., Elmquist, J.K., 2015. Loss of the liver X receptor LXRα/β in peripheral sensory neurons modifies energy expenditure. Elife. https://doi.org/10.7554/eLife.06667.

Nakagawa, T., Wakamatsu, K., Zhang, N., Maeda, S., Minami, M., Satoh, M., Kaneko, S., 2007. Intrathecal administration of ATP produces long-lasting allodynia in rats: differential mechanisms in the phase of the induction and maintenance. Neuroscience 147, 445–455.

Peng, Q., Liu, H., Shi, S., Li, M., 2014. Lycium ruthenicum polysaccharide attenuates inflammation through inhibiting TLR4/NF-kappaB signaling pathway. Int. J. Biol. Macromol. 67, 330–335.

Pourcet, B., Gage, M.C., Leon, T.E., Waddington, K.E., Pello, O.M., Steffensen, K.R., Castrillo, A., Valledor, A.F., Pineda-Torra, I., 2016. The nuclear receptor LXR modulates interleukin-18 levels in macrophages through multiple mechanisms. Sci. Rep. 6, 25481.

Rajendrasozhan, S., Yang, S.R., Kinnula, V.L., Rahman, I., 2008. SIRT1, an antiinflammatory and antiaging protein, is decreased in lungs of patients with chronic obstructive pulmonary disease. Am. J. Respir. Crit. Care Med. 177, 861–870.

Ramadori, G., Fujikawa, T., Anderson, J., Berglund, E.D., Frazao, R., Michan, S., Vianna, C.R., Sinclair, D.A., Elias, C.F., Coppari, R., 2011. SIRT1 deacetylase in SF1 neurons protects against metabolic imbalance. Cell Metabol. 14, 301–312.

Schuster, G.U., Parini, P., Wang, L., Alberti, S., Steffensen, K.R., Hansson, G.K., Angelin, B., Gustafsson, J.A., 2002. Accumulation of foam cells in liver X receptor-deficient mice. Circulation 106, 1147–1153.

Shao, H., Xue, Q., Zhang, F., Luo, Y., Zhu, H., Zhang, X., Zhang, H., Ding, W., Yu, B., 2014. Spinal SIRT1 activation attenuates neuropathic pain in mice. PLoS One 9, e100938.

Song, J., Ying, Y., Wang, W., Liu, X., Xu, X., Wei, X., Ruan, X., 2018. The role of P2X7R/ERK signaling in dorsal root ganglia satellite glial cells in the development of chronic postsurgical pain induced by skin/muscle incision and retraction (SMIR). Brain Behav. Immun. 69, 180–189.

Stellwagen, D., Beattie, E.C., Seo, J.Y., Malenka, R.C., 2005. Differential regulation of AMPA receptor and GABA receptor trafficking by tumor necrosis factor-alpha. J. Neurosci. 25, 3219–3228.

Tangirala, R.K., Bischoff, E.D., Joseph, S.B., Wagner, B.L., Walczak, R., Laffitte, B.A., Daige, C.L., Thomas, D., Heyman, R.A., Mangelsdorf, D.J., Wang, X., Lusis, A.J., Tontonoz, P., Schulman, I.G., 2002. Identification of macrophage liver X receptors as inhibitors of atherosclerosis. Proc. Natl. Acad. Sci. U. S. A. 99, 11896–11901.

Wang, B., Tontonoz, P., 2018. Liver X receptors in lipid signalling and membrane homeostasis. Nat. Rev. Endocrinol. 14, 452–463.

Xu, J., Feng, Y.W., Liu, L., Wang, W., Zhong, X.X., Wei, X.H., Liu, X.G., 2017. Liver X receptor alpha is involved in counteracting mechanical allodynia by inhibiting neuroinflammation in the spinal dorsal horn. Anesthesiology 127, 534–547.

Yang, T., Du, S., Liu, X., Ye, X., Wei, X., 2018. Withdrawal from spinal application of remifentanil induces long-term potentiation of c-fiber-evoked field potentials by activation of Src family kinases in spinal microglia. Neurochem. Res. 43, 1660–1670.

Yang, X.D., Tajkhorshid, E., Chen, L.F., 2010. Functional interplay between acetylation and methylation of the RelA subunit of NF-kappaB. Mol. Cell Biol. 30, 2170–2180.

Yeung, F., Hoberg, J.E., Ramsey, C.S., Keller, M.D., Jones, D.R., Frye, R.A., Mayo, M.W., 2004. Modulation of NF-kappaB-dependent transcription and cell survival by the SIRT1 deacetylase. EMBO J. 23, 2369–2380.

Yin, Q., Lu, F.F., Zhao, Y., Cheng, M.Y., Fan, Q., Cui, J., Liu, L., Cheng, W., Yan, C.D., 2013. Resveratrol facilitates pain attenuation in a rat model of neuropathic pain through the activation of spinal Sirt1. Reg. Anesth. Pain Med. 38, 93–99.

Ying, Y.L., Wei, X.H., Xu, X.B., She, S.Z., Zhou, L.J., Lv, J., Li, D., Zheng, B., Liu, X.G., 2014. Over-expression of P2X7 receptors in spinal glial cells contributes to the development of chronic postsurgical pain induced by skin/muscle incision and retraction (SMIR) in rats. Exp. Neurol. 261, 836–843.

Yuan, F., Chen, J., Sun, P.P., Guan, S., Xu, J., 2013. Wedelolactone inhibits LPS-induced pro-inflammation via NF-kappaB pathway in RAW 264.7 cells. J. Biomed. Sci. 20, 84.

Yuan, Y., Wang, J.Y., Yuan, F., Xie, K.L., Yu, Y.H., Wang, G.L., 2013. Glycogen synthase kinase-3 beta contributes to remifentanil-induced postoperative hyperalgesia via regulating N-methyl-D-aspartate receptor trafficking. Anesth. Analg. 116, 473–481.

Zhao, C., Dahlman-Wright, K., 2010. Liver X receptor in cholesterol metabolism. J. Endocrinol. 204, 233–240.

Zheng, Y., Hu, Q., Manaenko, A., Zhang, Y., Peng, Y., Xu, L., Tang, J., Tang, J., Zhang, J.H., 2015. 17 beta-Estradiol attenuates hematoma expansion through estrogen receptor alpha/silent information regulator 1/nuclear factor-kappa b pathway in hyperglycemic intracerebral hemorrhage mice. Stroke 46, 485–491.

Zhou, L.J., Zhong, Y., Ren, W.J., Li, Y.Y., Zhang, T., Liu, X.G., 2008. BDNF induces late-phase LTP of C-fiber evoked field potentials in rat spinal dorsal horn. Exp Neurol. 212, 507–514.

Zhou, L.J., Yang, T., Wei, X., Liu, Y., Xin, W.J., Chen, Y., Pang, R.P., Zang, Y., Li, Y.Y., Liu, X.G., 2011. Brain-derived neurotrophic factor contributes to spinal long-term potentiation and mechanical hypersensitivity by activation of spinal microglia in rat. Brain Behav Immun. 25, 322–334.

Zhou, C.H., Zhang, M.X., Zhou, S.S., Li, H., Gao, J., Du, L., Yin, X.X., 2017. SIRT1 attenuates neuropathic pain by epigenetic regulation of mGluR1/5 expressions in type 2 diabetic rats. Pain 158, 130–139.

Zeng, H.T., Fu, Y.C., Yu, W., Lin, J.M., Zhou, L., Liu, L., Wang, W., 2013. SIRT1 prevents atherosclerosis via liverXreceptor and NFkappaB signaling in a U937 cell model. Mol. Med. Rep. 8, 23–28.